GEOPHYSICAL RESEARCH LETTERS, VOL. 24, NO. 24, PAGES 3317-3320, DECEMBER 15, 1997

Synthetic seismograms through synthetic Franciscan: Insights into factors affecting large-aperture seismic data

Christof Lendl[1,2], Anne M. Tréhu[1], John A. Goff[3], Alan R. Levander[4], Bruce C. Beaudoin[5,6]

Abstract. In spite of an order of magnitude increase over the past 15 years in spatial sampling of the wavefield, a major uncertainty in the analysis of active source seismic data remains phase identification. This uncertainty results in part from the wide range of spatial scales of velocity heterogeneity in the crust. Smaller scale variations than those which can be deterministically resolved given the design of a particular seismic experiment can be modeled statistically using geologic constraints. Here we present synthetic seismograms generated from several different realizations of a stochastic model describing the velocity heterogeneity of Franciscan terrane rocks. We compare the results to observed data and to synthetic seismograms generated for a model derived from tomographic inversion of the data in order to obtain qualitative insights into the relative importance of large and small scale velocity heterogeneity. Not surprisingly, the synthetic data for the tomographic model best reproduce observed small-scale variations in first arrival time, which only occur for particular realizations of the stochastic model. The synthetic seismograms generated for the stochastic models best reproduce the level of signal-generated noise and suggest that the amplitude of velocity variation locally within the Franciscan is approximately 1 km/s. They also illustrate the effect of a strongly heterogeneous upper and mid-crust on the amplitude-versus-offset pattern of arrivals from the lower crust and upper mantle. These effects may sometimes be interpreted deterministically, leading to biased models or an overly optimistic estimate of lower crustal resolution.

Introduction

Most efforts to model large-aperture seismic data are based on matching the travel times of observed arrivals to travel times predicted by a model. In the past decade, considerable effort has been expended to improve methods for calculating travel-times and to develop inversion algorithms to automate the determination of the best-fitting model. These efforts have greatly increased the efficiency with which data can be modeled and have improved our understanding of the resolving capacity of the data. The resultant deterministic velocity models contain large blocks or layers within which velocity varies on a scale that is comparable to the larger of the source or receiver spacings. Although details of solutions depend somewhat on model parameterization, differences are decreasing between crustal models obtained independently by different groups using different methods to model the same data.

Much of this increased similarity between models is due to increases in data acquisition capability. An order of magnitude increase during the past decade in the spacing of traces within individual record sections (due in large part to acquisition of instruments by the IRIS PASSCAL program onshore and to the development of large-volume, tuned airgun arrays offshore) results in our improved ability to identify low amplitude and/or secondary phases. Decreased spacing of overlapping record sections (due to increased shot spacing onshore and to increased numbers of seafloor recorders offshore) results in improved resolution of lateral velocity variations. Nonetheless, identification of phases remains a major sources of uncertainty, and the uncertainly increases as the length of the raypath and geological complexity increase. Adequately incorporating the additional information on crustal structure provided by amplitude variations in the data also remains elusive for all but very simple models. In fact, our understanding of how seismic waves with wavelengths on the order of hundreds of meters propagate for hundreds of kilometers through the geologically complicated lithosphere remains quite poor. Observed seismic data generally contain a complicated coda, which is generally attributed to scattering [eg. *Menke and Chen*, 1984; *Frankel and Clayton*, 1986] and is not predicted by models derived from travel-times.

Several recent studies have attempted to characterize the elastic or acoustic properties of geologically complex materials in order to generate synthetic seismograms that reproduce some of the complexity observed in data. Maps of surface geology indicate that spatial variations in the elastic properties of the crust typically span length scales of several orders of magnitude [*Levander and Holliger*, 1992]. This variability can be described statistically using a small number of parameters, the values of which can be derived from geological maps and rock physics data. Details of the appropriate statistical model depend on the local geology. This approach has successfully reproduced characteristics of the coda in regions where the large-scale crustal velocity structure is relatively simple.

Here, we present the results of generating synthetic seismograms through a model of Franciscan accretionary complex rocks. Motivation was provided by the desire to understand how passage through very heterogeneous Franciscan accretionary complex rocks affects the wavefield and our ability to resolve details of underlying lithospheric structure in the region of the Mendocino triple junction (MTJ). A major active source seismic experiment (figure 1) was recently conducted in this region in order to image the subsurface geometry of the three lithospheric plates and provide constraints on geodynamic models of the effect of triple junction migration [*Trehu et al.*, 1995].

Stochastic Model Description

The Franciscan terrane of the MTJ region consists of turbidite and argillaceous sandstones, intermixed with numerous melange units that originated partly from large scale submarine mass flow deposits and partly from tectonic mixing in the subduction zone. The melange units contain blocks of graywacke, radiolarian chert, recrystallized limestone, blueschist facies metamorphic rock, greenstone, and plutonic rock of ophiolitic affinity [*Aalto*, 1994]. All these parts are strongly intermixed and form a highly complex structure. *Goff and Levander* [1996] derived a statistical description of Franciscan rocks that approximates the two main units of Franciscan rocks, sandstone (66%) and melange (34%),

[1]College of Oceanic and Atmos. Sci., Oregon State Un., Corvallis, OR
[2]Senckenberg Institute, Wilhelmshaven, Germany
[3]Un. of Texas Institute for Geophysics, Austin, TX
[4]Dept. of Geology and Geophysics, Rice Un., Houston, TX
[5]Dept of Geophysics, Stanford Un., Stanford, CA
[6]IRIS PASSCAL Instrument Center, Stanford, CA

Paper number 97GL03262.
0094-8534/97/97GL-03262$05.00

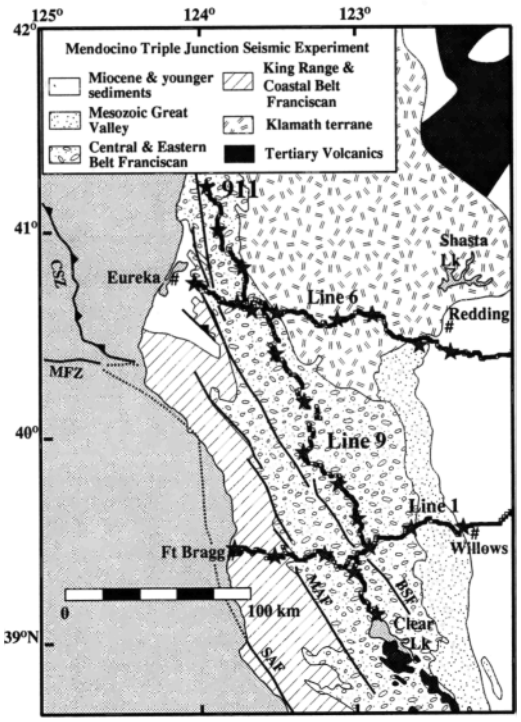

Figure 1. Simplified geologic map of northwestern California showing the location of the seismic profile that inspired this modeling effort. Shotpoints are shown as triangles; the shotpoint modeled in this paper (911) is labeled. SAF - San Andreas fault, MAF - Maacama fault, BSF - Bartlett Springs fault, CSZ - Cascadia subduction zone, MFZ - Mendocino fracture zone.

as a bimodal, approximately fractal, sinuously connected velocity distribution, with model parameters derived from digitized geological maps. The Franciscan is particularly interesting in that it is characterized by two distinct length scales and transverse anistropy. Characteristic vertical length scales are approximately 1.3 and 5.5 km, with horizontal scale larger by a factor of 2.75. We present synthetic seismograms for several different realizations of this velocity model and compare them to synthetic seismograms for deterministic velocity models.

Each realization of the stochastic model is represented by a binary grid in which values of +1 represent sandstone and values of -1 identify melange units. This is admittedly a gross simplification of velocity structure of the Franciscan terrane, as the melange is itself a very complex, heterogeneous medium. A grid spacing of 100 m was chosen to permit calculation of seismic waves with a frequency content of up to 5 Hz for velocities greater than 3 km/s. The values in the grid were then scaled to produce a specified maximum velocity difference that ranged from 0.5 to 1.5 km/s for different models. After scaling, the average velocity of the stochastic variations was removed from the grid to produce a mean value of 0, and the grid was masked to outline a region of Franciscan rocks in the model. Beneath the Franciscan, the value of the stochastic grid was 0.

The stochastic velocity grid was then added to a simple deterministic velocity grid determined from travel-time analysis of the data from line 9 of the Mendocino triple junction seismic experiment. Line 9 is located entirely within the Franciscan Coast Ranges of northwestern California (figure 1). For this study, the velocity within the Franciscan rocks was represented by a velocity of 3.0-4.0 km/s at the surface and of 6.5 km/s at the base of the Franciscan. This simple velocity structure represents the one-dimensional velocity model that provides the best fit to the observed first arrivals interpreted to represent P-waves refracted through the Franciscan rocks. Allowing for two-dimensional velocity variation in a tomographic inversion of first arrivals leads to a structure containing large "blobs" of higher or lower velocity in the upper 10 km [*Beaudoin et al.*, 1996].

Three different realizations of the stochastic P-wave velocity model are shown in figure 2a, as are the simple and tomographically-derived deterministic models. For each stochastic model, the peak-to-peak velocity difference in the stochastic grid is 1.0 km/s. For the lowermost crust and upper mantle, a model representing the crust of the subducted Gorda plate, which dips to the south and ends near km 80, was included in all models based on preliminary analysis of wide-angle reflections; south of km 80, a lower crust representing a tectonically or magmatically underplated mafic layer was included. This particular lower crustal model is not meant to represent a "final" model for line 9; it is included to illustrate the effect of the overlying stochastically heterogenous crust on signals from underlying structures. Although a general thickening of the crust in the central portion of line 9 is well determined from the data, details of the lower crust and upper mantle in this region are the subject of ongoing investigation.

Calculation of Synthetic Seismograms

Synthetic seismograms were calculated using an isotropic, elastic, 2-dimensional, staggered-grid, finite-difference algorithm to solve the wave equation. Three-dimensional versions of this algorithm have been discussed by *Rodrigues and Mora* [1992] and *Igel et al.* [1995]. The algorithm, which calculates eighth-order spatial derivatives using the method of *Holberg* [1987] and forth-order temporal derivatives through Taylor series truncation, has been implemented on a Connections Machine CM-5 at Oregon State University to permit calculation of synthetic seismograms and visualization of wavefield propagation through complicated 2-dimensional models derived from travel-time analysis of data from large-aperture active-source seismic experiments [Lendl, 1996].

In figure 2b, the observed data from a 2270 kg explosive shot [*Godfrey et al.*, 1995] located at the northern end of line 9 are compared to synthetic seismograms for seven different models: the simple deterministic model, the tomographic model, model R1 for peak-to-peak stochastic velocity variations of 0.5, 1.0 and 1.5 km/s, and models R2 and R3 for a peak-to-peak stochastic velocity variation 1 km/s. Models R1, R2 and R3 represent different realizations of the same stochastic model. All seismograms are displayed with a reduction velocity of 6.5 km/s and preserve relative amplitude variations as a function of both time and offset.

For the calculations, the density and elastic properties of the material, derived from P and S wave velocities, must be specified. P–velocity grids were created as discussed above. S–velocity and density grids were derived from the P–velocity grids assuming a Poisson's ratio of 0.25 and a fifth order polynomial fit to a compilation of laboratory velocity/density measurements [*Zelt and Smith*, 1992]. Results are not very sensitive to uncertainties in S-wave velocity or density [*Lendl*, 1996].

Stability and convergence of finite difference calculations depend on the proper choice of time step Δt and grid spacing Δx, which depend in turn on the lowest velocity in the model, the highest frequency in the source, and the algorithms used for spatial and temporal differentiation [*Levander*, 1989]. Theoretical considerations [*Rodrigues and Mora*, 1992; *Igel et al.*, 1995; *Lendl*, 1996] indicate that a grid spacing of at least 3 grid points/wavelength and $(c_p\Delta t)/(\Delta x) = 1.205$, where c_p is the largest P-wave velocity in the model, are adequate for stability of the algorithm used here. A series of simulations was done to test the domain of validity and determine an acceptable level of dispersion. The final choice was a grid spacing of 100 m and time steps of 0.01 s. The maximum frequency in the seismic

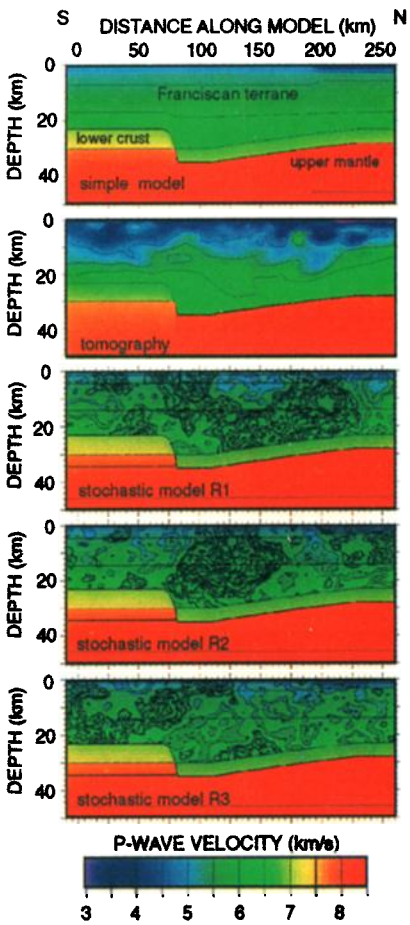

Figure 2 a. Velocity models.

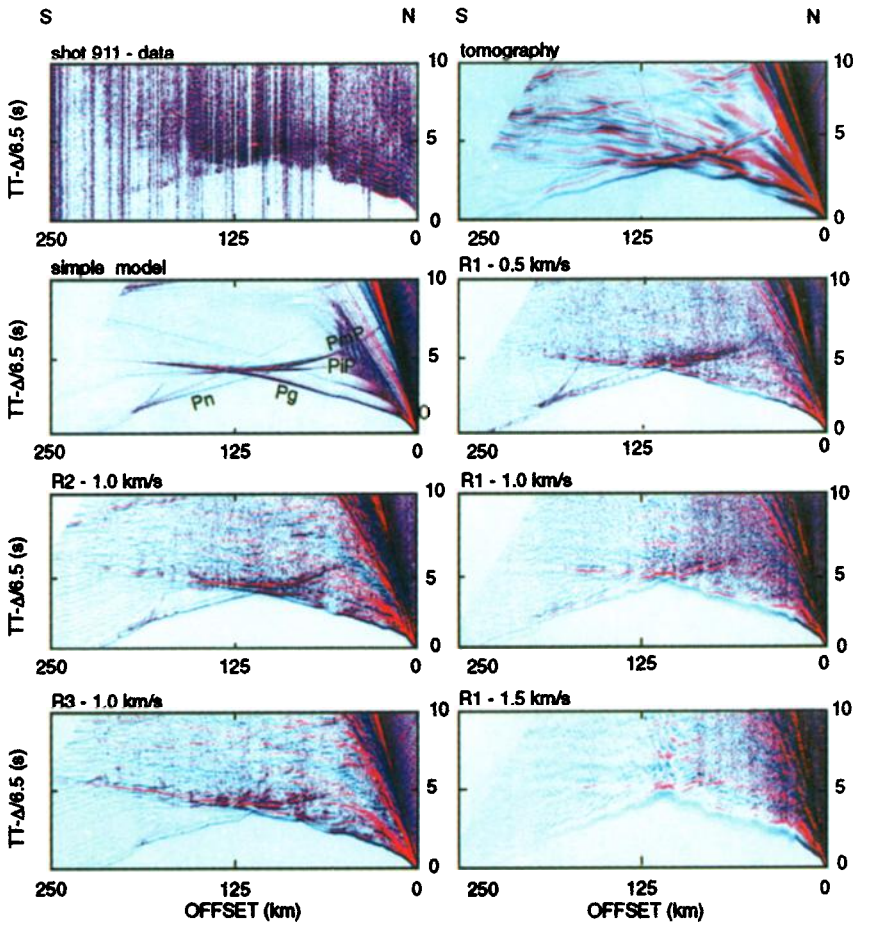

Figure 2b. Synthetic seismograms for the models of figure 2a compared to data for shot 911.

Figure 2a. Velocity models. Positions of shotpoints along the seismic profile are also shown. From top to bottom, the models are: the simple deterministic model; the tomographic inversion of first arrival times [*Beaudoin et al.,* 1996], modified to include the same lower crust as in the other models; three different realizations of the stochastic model, generated by using different random number seeds (see text). The amplitude of velocity variation for the stochastic models is 1 km/s.

Figure 2b. Observed data for shotpoint 911 compared to synthetic seismograms for the models shown in figure 2b and for different amplitudes of stochastic velocity variation. Several important phases have been labeled on the synthetics for the simple deterministic model: P_g - crustal diving wave; P_n - upper mantle interface head wave; PiP - reflection from the top of the lower crust layer; PmP - reflection from the base of the lower crustal layer. See text for further explanation.

source, which is defined by a Gaussian function, is 5 Hz. The synthetic seismograms for the simple deterministic model (figure 2b) give a qualitative idea of the level of numerical noise with these parameters. While the data contain higher frequencies, calculating synthetic data with such high frequencies for models the size required is beyond our current computing capabilities.

Absorbing boundary conditions are implemented on the sides and bottom of the model by extending the model and multiplying displacement amplitudes within this region by an absorbtion factor that decreases exponentially within this boundary region [*Cerjan et al.,* 1985]. For the synthetics shown here, the top of the model acts as free surface. Because the near-surface velocities in the model are considerably higher than velocities measured near the surface along line 9 (again because of computational limitations), and because intrinsic attenuation is not included, strong surface waves appear in the synthetics that are not apparent in the data.

Discussion

One feature of the data (figure 2b), which is generally characteristic of data collected within the Franciscan terrane, is the strong "background" noise following the first arrivals. This noise must be signal-generated. Also characteristic are the large variations in the amplitude of the signal, with strong secondary arrivals observed locally that cannot be readily identified. These features are not observed in the synthetic seismograms for the simple deterministic model. While the synthetic seismograms for the model derived deterministically via tomographic inversion of the first arrivals accurately reproduce the variable apparent velocity of the first arrivals, the focussing and defocussing of energy in the P_g arrival and in the following one or two seconds is exaggerated. This model also does not reproduce the observed level of background signal-generated noise.

Comparing the seismograms for the simple deterministic model to those for stochastic model R1 with different peak-to-peak stochastic velocity variations, we see that, not surprisingly, the seismograms for the stochastic models show considerable energy following the first arrivals. For velocity variations of 0.5 km/s, the background scattering level is distributed homogeneously along the whole profile. With increasing stochastic velocity contrast, strong frequency-dependent attenuation is observed with increasing offset. Other effects of the increased scattering are that weaker arrivals disappear into the "background" signal-generated noise and that the details of travel-

time triplications are obscured. The model with a 1.0 km/s stochastic velocity variation produces synthetic seismograms that, qualitatively, most resemble the observations. However, because the source for the synthetic seismograms does not contain frequencies above 5 Hz whereas the real source does and because scattering in the model is two-dimensional whereas scattering in the earth is three-dimensional, quantitative estimations of the amplitude of velocity variation and attenuation in the Franciscan terrane from these simulations are not justified.

We also compared synthetic seismograms for several different realizations of the same stochastic model (i.e. models derived using the same background deterministic model and the same statistical parameters to define velocity variation within the Franciscan terrane). The seismic sections generated in this way show similarities and differences. For example, the character of the crustal diving wave (P_g) is different for the different realizations. The seismic sections for R1 and R2 show the P_g arrival continuing smoothly with an approximately constant apparent velocity from offsets of 25-110 km, where P_g is overtaken by the P_n arrival. Amplitude modulation and secondary arrivals that closely follow P_g are somewhat different for these two realizations. In contrast, the P_g arrival for R3 shows larger variations of apparent velocity and greater amplitude modulation, similar to the observations and to the synthetic seismograms generated for the tomographic inversion model.

The apparent amplitude versus offset (AVO) behavior of the wide-angle reflection from the base of the crust (PmP) also is different for the three realizations. For R1 and R3, PmP is observed for offsets of 60-210 km, but the character of this phase is different. R1 shows two large "shingles" at 140-160 km offsets, whereas R3 shows smaller "shingles" at offsets of 75-120 km. R2 does not show "shingles" and PmP is delayed beyond offsets of about 160 km. In addition, a strong phase precedes PmP at offsets of 80-110 km on R2 (and in the data), but is not visible on R1 and R3.

The differences among the synthetic seismic sections generated for three different realizations of the same stochastic model obviously depend on the spatial distribution of the stochastic velocity variations. In areas of dominantly large-scale velocity variations, the wavefronts are broken into separately distinguishable wavefronts, and strong traveltime variations and amplitude modulation result. Areas of dominantly small-scale variations, on the other hand, scatter the wavefront and create an envelope of energy. Wavefronts for R3 travel almost exclusively through areas with large-scale velocity variations, whereas wavefronts for R1, travel primarily through a region of small-scale variations for the raypaths of phases discussed above. It should be noted that the same variations would be generated for different shotpoint locations and a single model realization, perhaps explaining observed AVO differences for a given phase from different shotpoints in active source seismic data. Such variations are sometimes interpreted as the signature of lower crust and upper mantle structure whereas these results show that they may be produced by amplitude variations within the upper and mid-crust.

We conclude that the success of this initial effort at simulating wave propogation for distances of 100s of km through complicated crustal models suggests that future efforts to extract information on small-scale crustal heterogeneity directly from the data [*Pullammanappallil et al.*, 1997] should be fruitful. This information can then be used to compensate for small-scale effects when modeling traveling times to derive large-scale lithospheric structure.

Acknowledgements. Many thanks to those who made the Mendocino triple junction seismic experiment possible, including the many instrument deployers and the IRIS/PASSCAL, USGS, and Lithoprobe instrument centers, which furnished instruments for the data acquisition. Thanks also to Peter Mora for providing the finite difference modeling algorithm, and to Mark Abbott and the NASA Earth Observing System program for providing the CM-5 supercomputer that made the calculations possible. Tom Brocher and an anonymous reviewer provided helpful comments. Figures were constructed using GMT [*Wessel and Smith*, 1995]. This project was funded by the Continental Dynamics program of the National Science Foundation through grants EAR-9219870 and EAR-9527001.

References

Aalto, K. R., Late Cenozoic sediment provenance and tectonic evolution of the northernmost Coast Ranges, California, Penrose Conference, Eureka, CA, *Guidebook Penrose Field Trip*, 73-89, 1994.

Beaudoin, B. C., N. J. Godfrey, S. L. Klemperer, C. Lendl, A. M. Tréhu, T. J. Henstock, A. R. Levander, J. E. Holl, A. S. Meltzer, J. H. Luetgert, and W. D. Mooney, The transition from slab to slabless: Results from the 1993 Mendocino Triple Junction seismic experiment, *Geology, 24*, 195-199, 1996.

Cerjan, C., D. Kosloff, R. Kosloff and M. Reshef, A non-reflecting boundary condition for discrete acoustic and elastic wave equations, *Geophysics, 50*, 705-708, 1985.

Frankel, A., and R. W. Clayton, Finite difference simulations of seismic scattering: implications for the propagation of short-period seismic waves in the crust and models of crustal heterogeneity, *J. Geophys. Res., 91*, 6465-6489, 1986.

Godfrey, J. J., B. C. Beaudoin, C. Lendl, A. Meltzer, and J. Luetgert, Data report for the 1993 Mendocino triple junction seismic experiment, *Open-File Report 95-275*, U. S. Geological Survey, 83 pp., 1995.

Goff, J. A., and A. R. Levander, Incorporating "sinuous connectivity" into stochastic models of crustal heterogeneity: Examples from the Lewisian gneiss complex, Scotland, the Franciscian formation, California, and the Hafafit gneiss complex, Egypt., *J. Geophys. Res., 101*, 8489-8502, 1996.

Holberg, O., Computational aspects of the choice of operator and sampling interval for numerical differentiation in large-scale simulation of wave phenomena, *Geophys. Prospecting, 35*, 629-655, 1987.

Igel, H., P. Mora, B. Riollet, Anisotropic propagation through finite-difference grids, *Geophysics, 60*, 1203-1216, 1995.

Lendl, C., Finite difference wavefield modeling of large-aperture data from the 1993 Mendocino triple junction seismic experiment, M.S. thesis, 163 pp., Oregon State Un., 1996.

Levander, A. R., Finite-difference forward modeling in seismology, in *The Encyclopedia of Solid Earth Geophysics*, edited by D. James, pp. 410-431, Van-Nostrand-Reinhold, 1989.

Levander , A. R., and K. Holliger, Small scale heterogeneity and large-scale velocity structure of the continental crust, *J. Geophys. Res., 97*, 8797-8804, 1992.

Menke, W., and R. Chen, Numerical studies of the coda fall-off rate of multiply-scattered waves in randomly layered media, *Bull. Seis. Soc. Am., 74*, 1079-1081, 1984.

Pullammanappallil, S., A. Levander, and S. P. Larkin, Determination of crustal stochastic parameters from seismic exploration data, *J. Geophys. Res., 102*, 15269-15286, 1997.

Rodrigues, D., and P. Mora, Analysis of a finite difference solution to the three-dimensional elastic wave equation, 62nd Ann. Int. Mtg., *Soc. Expl. Geophys., Expanded Abstracts*, 1247-1249, 1992.

Tréhu, A. M., and Mendocino Working Group, Pulling the rug out from under California: Seismic images of the Mendocino Triple Junction region, *Eos Trans AGU, 76 (38)*, 369, 1995.

Wessel, P., and W. H. F. Smith, New version of the generic mapping tools released, *Eos Trans AGU, 76 (33)*, 329, 1995.

Zelt, C. A., and R. B. Smith, Seismic traveltime inversion for 2-D crustal velocity structure, *Geophys. J. Int., 108*, 16-34, 1992.

C. Lendl, Senckenberg Institute, Schleusenstr. 39A, D-26382, Wilhelmshaven, Germany.

A. M. Tréhu (corresponding author), College of Oceanic and Atmospheric Sciences, Oregon State University, 104 Ocean Admin Bldg., Corvallis, OR 97331-5503 (e-mail: trehu@oce.orst.edu).

J. A. Goff, Un. of Texas Institute for Geophysics, Austin, TX.

A. R. Levander, Dept. of Geology and Geophysics, Rice Un., Houston, TX.

B. C. Beaudoin, IRIS PASSCAL Instrument Center, Stanford, CA.

(Received March 18, 1997; revised October 3, 1997; accepted October 29, 1997).